CONF-800661--1

LA-UR -80-1633

TITLE: NUMERICAL SIMULATION OF REACTIVE FLOW IN INTERNAL COMBUSTION ENGINES

AUTHOR(S): L. D. Cloutman
J. K. Dukowicz
J. D. Ramshaw

SUBMITTED TO: To be published in the Proceedings of the Seventh International Conference on Numerical Methods in Fluid Dynamics, Stanford University/NASA Ames, June 23-27, 1980

University of California
LOS ALAMOS SCIENTIFIC LABORATORY
Post Office Box 1663 Los Alamos, New Mexico 87545
An Affirmative Action/Equal Opportunity Employer

Form No. 836 R3
St. No. 2629
12/78

UNITED STATES
DEPARTMENT OF ENERGY
CONTRACT W-7405-ENG-36

NUMERICAL SIMULATION OF REACTIVE FLOW IN INTERNAL COMBUSTION ENGINES

L. D. Cloutman, J. K. Dukowicz and J. D. Ramshaw
Theoretical Division, Group T-3
Los Alamos Scientific Laboratory
University of California
Los Alamos, NM 87545

I. INTRODUCTION

Multidimensional numerical simulations of the reactive fluid flow in an internal combustion engine cylinder are useful in helping engine designers obtain insight into the physical mechanisms governing efficiency and pollutant formation. For background information and references to other work in this area, the reader is referred to the proceedings of a recent symposium (Mattavi and Amann 1980). This paper describes a comprehensive numerical model for internal combustion engine cylinder simulations that has been developed at Los Alamos. The model is currently embodied in a two-dimensional (axisymmetric) computer code called CONCHAS-SPRAY. Work is in progress on a three-dimensional code with the same features. A detailed discussion of all aspects of the model would be inappropriate here. We therefore emphasize selected topics of particular interest. More detailed discussions of some of these topics are available elsewhere (Butler et al. 1979, Dukowicz 1979, Dukowicz 1980, Ramshaw and Cloutman 1980).

II. FINITE-DIFFERENCE PROCEDURE

The fluid dynamical part of our model is a time-marching finite-difference procedure that is based on the combined use of the ICE (implicit continuous-fluid Eulerian) and ALE (arbitrary Lagrangian-Eulerian) methods. The ICE method (Harlow and Amsden 1971) is a partially implicit temporal differencing procedure in which the pressure gradient in the momentum equation and the divergence term in the continuity equation are simultaneously evaluated at the advanced time level. This procedure removes the Courant sound-speed stability restriction on the time step, thereby allowing the efficient computation of flow at low Mach number. The ALE method (Trulio 1966; Hirt, Amsden, and Cook 1974) is a spatial differencing procedure that utilizes a mesh composed of arbitrary quadrilaterals whose corner locations may be arbitrarily specified as functions of time. This method allows the convenient representation of curved and/or moving boundary surfaces, such as the moving piston.

The implicit part of the ICE scheme obtains the advanced time pressure and velocity fields by an iterative procedure similar to the method of successive over-relaxation. Such methods are notoriously inefficient in effecting a change in the overall pressure level, because of the intrinsically slow relaxation of long wavelength errors. (The relaxation rate goes to zero as the square of the wave number.) This is a serious drawback in the present context, where substantial changes in the pressure level result both from the essentially adiabatic compression caused by the piston motion, and from the heat release that accompanies the combustion of the fuel. It was therefore necessary to develop a special technique to accelerate the iteration procedure.

The basic idea of the iteration acceleration technique is to estimate the change Δp in the overall pressure level that will occur on the time step in question, and to add that change into the entire pressure field at the beginning of the iteration procedure. In the present scheme, the advancement of the dependent variables through a time step is computed in three stages. The first stage is an explicit Lagrangian calculation, during which the heat release due to chemistry and/or phase change occurs. The second stage is the pressure iteration. The third stage is the rezone calculation, during which the mesh points are moved to their final locations and the associated transport is computed. Since the pressure iteration is Lagran-

gian and isentropic, overall pressure levels are obtained by a Lagrangian isentropic pressure equilibration within the constraint of the available total volume. We thereby obtain the formula

$$\bar{p} = \left[\frac{1}{V}\sum_{ij}\left(p_{ij}^{0}\right)^{1/\gamma} V_{ij}^{0}\right]^{\gamma} \qquad (1)$$

for the pressure level $\bar{p}$, where γ is the specific heat ratio, p_{ij}^{0} and V_{ij}^{0} are the pressure and volume of cell ij prior to equilibration, and V is the total volume in which the equilibration occurs. This formula neglects spatial variations in γ, which is a reasonable approximation that was necessary to obtain $\bar{p}$ in closed form. The pressure change Δp is estimated by $\bar{p}^{I} - \bar{p}^{n}$, where superscripts n and I refer respectively to the previous time level and to the first stage of the current time step.

Another problem of efficiency arises in connection with the finite-difference cells in the "squish region" between the piston face and the cylinder head. As the piston approaches top dead center, these cells become very small and the explicit diffusional stability limit on the time step becomes very restrictive. This problem is avoided by means of a "chopper" algorithm which automatically combines smaller cells into larger ones once a certain mimimum cell size is reached. The mass, momentum, and energy of the original cells are apportioned among the new cells in a conservative manner. As the piston recedes from top dead center, the inverse procedure is used to restore the original cells again.

III. BOUNDARY LAYER TREATMENT

Under most circumstances, the velocity and temperature boundary layers in an engine cylinder will be too thin to be explicitly resolved in a practical computing mesh. Since these boundary layers will ordinarily be turbulent, this difficulty may be circumvented by matching to the turbulent law of the wall (e.g., Schlichting 1968), which may be written in the form

$$\frac{u}{u_{*}} = \frac{1}{K}\,\ell n\left(\frac{y u_{*}}{\nu}\right) + B \quad . \qquad (2)$$

Here u is the magnitude of the fluid velocity at a perpendicular distance y from the wall, ν is the kinematic viscosity, $K \simeq 0.41$ is the Karman constant, B is a constant that depends on wall roughness (for a smooth wall, $B = 5.5$), and u_{*} is the shear speed, which is related to the wall shear stress τ and the density ρ by $\tau = \rho u_{*}^{2}$. To apply Eq. (2) in a finite-difference calculation, one assumes that the first mesh point away from the wall lies in the law-of-the-wall region. The values of u and y at this point are then substituted into Eq. (2); this determines u_{*} and hence τ. The value of τ thus determined is then imposed as a boundary condition.

Unfortunately, Eq. (2) is a transcendental equation for u_{*}, and this is not very convenient. We therefore use an approximation to Eq. (2) obtained by replacing u_{*} in the argument of the logarithm with its 1/7-law value. For a smooth wall, this yields

$$\frac{u}{u_{*}} = 2.19\,\ell n\left(\frac{y u}{\nu}\right) + 0.75 \quad , \qquad (3)$$

which is almost as accurate as Eq. (2) and can be solved explicitly for u_{*}.

The thermal boundary layer is handled in a similar way using the modified Reynolds analogy formula

$$q = \frac{1}{Pr_t}\left(\frac{\tau}{u}\right) C_p (T - T_w) \quad . \tag{4}$$

Here q is the heat flux to the wall, C_p is the specific heat at constant pressure, T_w is the wall temperature, T is the fluid temperature at the location of u, and $Pr_t \cong 0.89$ is the turbulent Prandtl number. Equation (4) may be obtained in a variety of ways; here we merely note that it results from appropriate simplification of a formula used by Launder and Spalding (1974).

IV. CHEMICAL REACTIONS

A ubiquitous problem in reactive fluid dynamics is the presence of chemical time scales that are very short in comparison to typical fluid dynamical characteristic times. The temporal resolution of these short time scales would require the use of impractically small time steps. This problem may be circumvented by assuming that the fast reactions are always in equilibrium, while the slower reactions proceed kinetically (Ramshaw 1980). In the present scheme, the kinetic reactions are treated by a linearly implicit procedure used in earlier reactive fluid dynamics codes (Rivard, Farmer, and Butler 1975, Ramshaw and Dukowicz 1979), while the equilibrium reactions are treated by a new quadratic iterative procedure (Ramshaw and Cloutman 1980). The latter procedure enforces the equilibrium constraints on the species concentrations by computing a sequence of progress increments in the equilibrium reactions. Each such increment is based on the instantaneous deviation of the corresponding reaction from equilibrium, and attempts to nullify this deviation. The procedure converges rapidly because the deviations from equilibrium are of the order of the time step, except perhaps at the beginning of the calculation.

V. PARTICLE-FLUID MODEL FOR EVAPORATING FUEL SPRAYS

Fuel-injected internal combustion engines typically employ injectors producing finely atomized sprays with complex distribution patterns and time-varying injection rates. Such strongly interacting, transient sprays are difficult to model using conventional techniques. The difficulties stem from the fact that the spray contains a wide range of droplet sizes, length scales, and time scales.

Our approach is based on a Monte Carlo statistical model. The injector distributions in droplet size, velocity, etc., are statistically sampled and these discrete droplets are followed along Lagrangian trajectories as they interact with the surrounding gas. Each computational droplet represents a number of similar physical droplets. The fundamental advantage of this approach is that all relevant time and spatial scales can be resolved in a computationally efficient manner, since the number of particles required for satisfactory accuracy is not excessive.

The following description will be limited to the essential features of the method. Additional details may be found elsewhere (Dukowicz 1979, 1980). The droplets interact with the gas by interchange of mass, momentum, and energy. Volume displacement effects are neglected for simplicity. We have also neglected the droplet-droplet interactions which would occur in a thick spray. In spite of the assumption of thin sprays (void fraction $\cong 1$), the spray may contain a large amount of mass and momentum compared to the gas, because of the large ratio of liquid to gas density. Thus the spray can strongly affect the gas flow, and vice versa. Further, because of the rapid rates of exchange of momentum and energy of small droplets, the coupling with the gas must be implicit. The required iteration for momentum coupling can fortunately be incorporated into the ICE pressure iteration so that essentially no additional computation is required.

An important property of sprays is the turbulent diffusion of droplets. This is modeled by a random choice method in which turbulent velocity components are added to the gas velocities, which in turn produce turbulent droplet velocities. This requires the turbulence intensity and length scales (or time scales) to be specified.

Phase change (primarily evaporation) is based on a quasi-steady evaporation model. The evolution of each droplet's temperature and radius is followed in time. At the present time, droplet internal motions and temperature distributions are ignored. Droplets affect each other during evaporation by modifying the ambient vapor density and gas temperature. This is modeled by evaporating droplets sequentially, assuming an isentropic, constant pressure process in each cell. The sequence of droplet evaporation is shuffled randomly on each time step. The resulting mass and internal energy changes are then added to each cell prior to the isentropic pressure iteration.

VI. SAMPLE CALCULATION

The sample calculation is a typical simulation of a direct injection stratified charge (DISC) engine. On the intake stroke, pure air is drawn into the cylinder through a shrouded valve, causing the air to swirl about the center line of the cylinder. At some point during the compression stroke, liquid fuel (n-octane in this example) is sprayed into the cylinder, followed by ignition near top dead center. Conventional power and exhaust strokes follow. In our example, the bore is 9.844 cm, the stroke is 9.55 cm, the compression ratio is 10:1, the swirl ratio is 4:1, the engine speed is 1600 rpm, and the cup in the piston has a diameter of 4.92 cm and a depth of 3.34 cm. The calculation is started at the beginning of the compression stroke with the air at 0.097 MPa and 308 K, corresponding to a highly loaded engine. Because the model is axisymmetric, the fuel injector and spark plug are located at the same point in the center of the cylinder head.

Typical computational results are shown in Figures 1 and 2. At 15.4 ms after bottom dead center (ABDC) on the compression stroke, liquid n-octane is injected into the compressed air. The left panel of Figure 1 shows the gas velocity at 16.65 ms. The incoming droplets entrain the air and create a downward jet along the symmetry axis. Air is also being pushed out of the squish region to the right by the upward motion of the piston. The dotted lines are contours of three different values of the swirl velocity. Air entrained by the entering droplets is pulled toward the axis, creating a region of high swirl, denoted by H, near the injector orfice. Radial transport of angular momentum in the squish region plus boundary layer drag produce a local high swirl rate at the entrance to the squish region, with a lower swirl rate inside.

The right hand panel of Figure 1 shows the droplets in the spray and contours of equivalence ratio. The central contour is the location of a stoichiometric mixture, and the left and right contours correspond approximately to the rich and lean flammability limits, respectively. Most of the droplets are small and confined to the core of the spray, where their evaporation contributes to fuel rich conditions. The droplets outside the contours are a few large ones (up to 30 μm) that couple loosely to the gas.

At 16.9 ms injection ends. Ignition at the injector orifice is at 17.1 ms. Figure 2 shows the solution at 19.11 ms. The left hand panel shows isotherms (solid lines) and mass fraction of NO (dashed lines). The band of high temperature shows where the flame has passed as it traveled down the flammable region at the edge of the spray. At this time, the flame has not reached the tip of the spray. The dashed lines show mass fractions of NO, with the highest value near the H. At all times, the regions that have been hottest for the longest contain the most NO.

Some of the droplets persist, as shown in the right hand panel of Figure 2. The droplets away from the axis evaporate quickly as the flame approaches. The particles near the axis evaporate very slowly because of the low temperature and high fuel vapor concentration. The ragged character of the equivalence ratio contours is an artifact of having tiny oxygen and fuel concentrations along the upper two thirds of the mesh. These contours show the sharp separation between the oxygen and fuel. The temperature is high in this region indicating the presence of a slowly burning diffusion flame.

REFERENCES

Butler, T. D., Cloutman, L. D., Dukowicz, J. K., and Ramshaw, J. D. 1979, "CONCHAS: An Arbitrary Lagrangian-Eulerian Computer Code for Multicomponent Chemically Reactive Fluid Flow at All Speeds," Los Alamos Scientific Laboratory report LA-8129-MS.

Dukowicz, J. K. 1979, "Quasi-Steady Droplet Phase Change in the Presence of Convection," Los Alamos Scientific Laboratory report LA-7997-MS.

Dukowicz, J. K. 1980, J. Comp. Phys. 35, 229.

Harlow, F. H. and Amsden, A. A. 1971, J. Comp. Phys. 8, 197.

Hirt, C. W., Amsden, A. A., and Cook, J. L. 1974, J. Comp. Phys. 14, 227.

Launder, B. E. and Spalding, D. B. 1974, Comp. Meths. Appl. Mech. Eng. 3, 269.

Mattavi, J. N. and Amann, C. A., eds. 1980, Combustion Modeling in Reciprocating Engines, Phenum Press, New York.

Ramshaw, J. D. and Dukowicz, J. K. 1979, "APACHE: A Generalized-Mesh Eulerian Computer Code for Multicomponent Chemically Reactive Fluid Flow," Los Alamos Scientific Laboratory report LA-7427.

Ramshaw, J. D. 1980, Phys. Fluids 23, 675.

Ramshaw, J. D. and Cloutman, L. D. 1980, "Numerical Method for Partial Equilibrium Flow," J. Comp Phys., in press.

Rivard, W. C., Farmer, O. A., and Butler, T. D. 1975, "RICE: A Computer Program for Multicomponent Chemically Reactive Flows at All Speeds," Los Alamos Scientific Laboratory report LA-5812.

Schlichting, H. 1968, Boundary-Layer Theory, 6th ed., McGraw-Hill, New York.

Trulio, J. G. 1966, "Theory and Structure of the AFTON Codes," Air Force Weapons Laboratory report AFWL-TR-66-19.

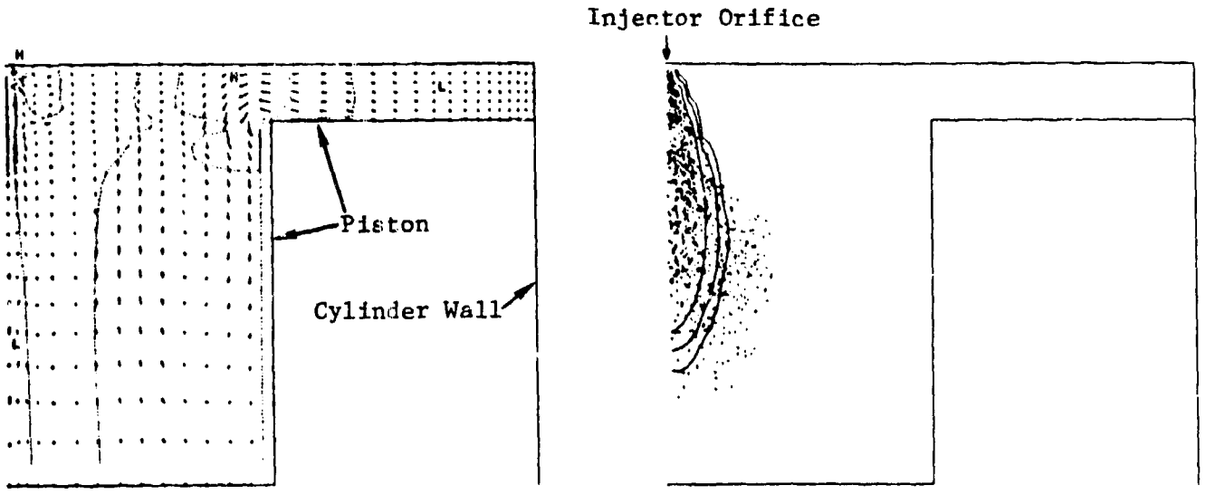

Fig. 1. The solution at 16.65 ms ABDC. The top of each panel is the cylinder head, and the left hand side is the symmetry axis. Maximum speed in the velocity vector plot is 4338 cm s^{-1}. The swirl velocity contours (dotted lines) have values of 1635, 3563, and 5492 cm s^{-1}, and the maximum value is 6777 cm s^{-1}. In the spray plot, the contours of equivalence ratio have values of 2, 1, and ½ from left to right.

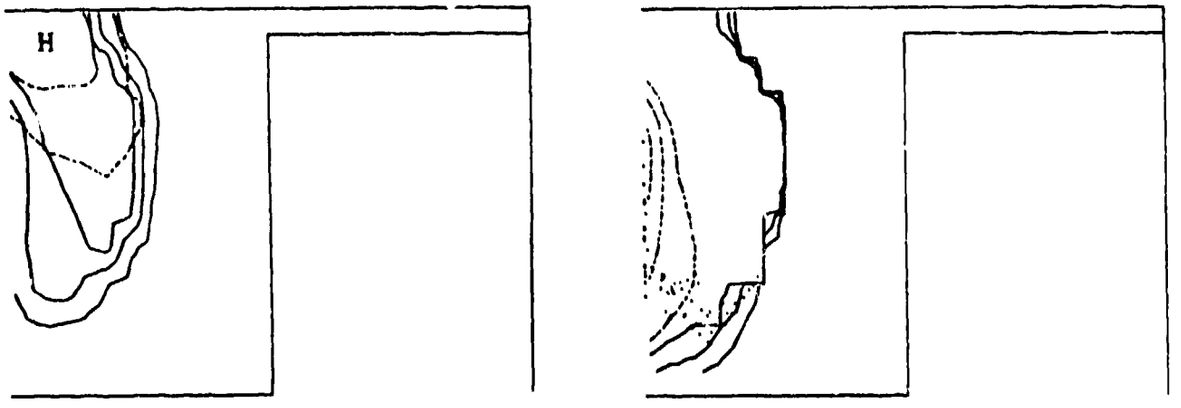

Fig. 2. The solution at 19.11 ms ABDC. The left panel shows isotherms (solid lines with values of 1000, 1500, and 2000 K and NO mass fraction concours (dashed lines) with values of 1×10^{-5} and 2×10^{-5}. The temperature reaches a maximum of 2316 K, and the NO mass fraction reaches a maximum of 2.6×10^{-5} at the H. In the right hand panel, a few droplets persist. The solid lines are are equivalence ratio contours with values of 2, 1, and ½ from left to right. The dashed lines are contours of fuel mass fraction with values of 0.3, 0.2, and 0.1 from left to right.